Squeezed-light spin noise spectroscopy

Vito Giovanni Lucivero,[1,*] Ricardo Jiménez-Martínez,[1] Jia Kong,[1] and Morgan W. Mitchell[1,2]

[1]*ICFO-Institut de Ciencies Fotoniques, Barcelona Institute of Science and Technology, 08860 Castelldefels (Barcelona), Spain*

[2]*ICREA-Institució Catalana de Recerca i Estudis Avançats, 08015 Barcelona, Spain*

We report quantum enhancement of Faraday rotation spin noise spectroscopy by polarization squeezing of the probe beam. Using natural abundance Rb in 100 Torr of N_2 buffer gas and squeezed light from a subthreshold optical parametric oscillator stabilized 20 GHz to the blue of the D_1 resonance, we observe that an input squeezing of 3.0 dB improves the signal-to-noise ratio by 1.5 to 2.6 dB over the combined (power)⊗(number density) ranges (0.5–4.0 mW)⊗(1.5×10^{12} cm^{-3} to 1.3×10^{13} cm^{-3}), covering the ranges used in optimized spin noise spectroscopy experiments. We also show that squeezing improves the tradeoff between statistical sensitivity and broadening effects, a previously unobserved quantum advantage.

I. INTRODUCTION

The presence of intrinsic fluctuations of a spin system in thermal equilibrium was first predicted by Bloch [1] and experimentally demonstrated in the 1980's by Aleksandrov and Zapasskii [2]. In the last decade, spin noise spectroscopy (SNS) has emerged as a powerful technique for determining physical properties of an *unperturbed* spin system from its noise power spectrum [3,4]. SNS has allowed the measurement of *g* factors, nuclear spin, isotope abundance ratios, and relaxation rates of alkali-metal atoms [5,6]; *g* factors, relaxation times, and doping concentration of electrons in semiconductors [7–11]; and localized holes in quantum dot ensembles [12,13] including single-hole spin detection [14]. Recently, SNS has been used to study complex optical transitions and broadening processes [15,16], coherent phenomena beyond linear response [17], and cross correlations of heterogeneous spin systems [18,19].

Spin noise has been measured with nuclear magnetic resonance [20,21] and magnetic force microscopy [22–24], but the most sensitive and widely used detection technique is Faraday rotation (FR) [2,5,6], in which the spin noise is mapped onto the polarization of an off-resonant probe. In FR-SNS, spin noise near the Larmor frequency competes with quantum noise [25] of the detected photons, i.e., the optical shot noise. The main figure of merit is η, the peak power spectral density (PSD) due to spin noise over the PSD due to shot noise, called "signal strength" [26] or the "signal-to-noise ratio" (SNR). Reported SNRs for single-pass atomic ensembles range from 0 to 13 dB [5,27], and up to 21 dB in atomic multipass cells [28]. Due to weaker coupling to the probe beam, reported SNRs range from −50 to −20 dB in semiconductor systems (see Table I in [26]). Several works have studied how to improve the polarimetric sensitivity [29] or to cancel technical noise sources [7,8,10], but without altering the fundamental tradeoff between sensitivity and broadening processes [29].

For small optical power P and atomic density n, SNR is linear in each: $\eta \propto nP$. At higher values, light scattering and atomic collisions broaden the spin noise resonances, and thus introduce systematic errors in measurements,

e.g., of relaxation rates, that are derived from the SNS linewidth [5–7]. This tradeoff between statistical sensitivity and line broadening is a fundamental limitation of the technique, with its origin in quantum noise properties of the atomic and optical parts of the system.

Here we work in a high-density regime, with atomic number densities up to $n \sim 10^{13}$ cm^{-3}, covering the range of recent experiments with optimized atomic instruments [5,6,18,27]. Earlier studies in this regime have observed nontrivial interactions between optical quantum noise and nonlinear magneto-optical rotation (NMOR) of an on-resonance probe [30] including increased measurement noise as a result of input squeezing for densities above $n \approx 2 \times 10^{11}$ cm^{-3} [31]. It is thus not obvious that squeezing will improve a high-density Faraday rotation measurement [3,32], as it does for lower densities [25,33]. In contrast, here we observe that squeezing does in fact improve both the signal-to-noise ratio and the tradeoff between sensitivity and line-broadening in SNS, over the full practical range of the technique. It is worth noting that we work with an unpolarized atomic ensemble and off-resonant probing, as required for the nonperturbative SNS technique. This may explain the difference between our results and prior experiments [30,31].

II. THEORY

As described in detail in the Appendix, FR optical probing gives a signal proportional to the on-axis projection of the collective spin of a group of atoms in thermal equilibrium. The collective spin precesses in response to external magnetic fields and experiences a stochastic motion as required by the fluctuation-dissipation theorem [2,26]. For rubidium, which has two isotopes, ^{85}Rb and ^{87}Rb, and shot-noise limited detection [34], the power spectrum of the FR signal is given by a double Lorentzian function:

$$S(\nu) = S_{\text{ph}} + \sum_{i \in \{85,87\}} S_{\text{at}}^{(i)} \frac{(\Delta \nu_i/2)^2}{\left(\nu - \nu_L^{(i)}\right)^2 + (\Delta \nu_i/2)^2}, \quad (1)$$

where $S_{\text{ph}} \propto P\xi^2$ is the (frequency-independent) shot-noise contribution at power P and ξ^2 is the squeezing factor. The sum on i is over the atomic mass, $\nu_L^{(i)}$ and $\Delta \nu_i$ are the (linear) Larmor frequency and FWHM width, respectively. $S_{\text{at}}^{(i)}$ is the

*vito-giovanni.lucivero@icfo.es

height of Lorentzian spin noise contribution. The SNR is

$$\eta_i \equiv \frac{S_{\text{at}}^{(i)}}{S_{\text{ph}}} = \frac{P}{\hbar\omega} \frac{4Q}{\xi^2} \frac{\sigma_0^2}{A_{\text{eff}}^2} \frac{\kappa_i^2 n_i L_{\text{cell}} A_{\text{eff}}}{\Gamma}, \quad (2)$$

where $\hbar\omega$ is the photon energy, Q is the quantum efficiency, σ_0 is the resonant optical cross section of the collision-broadened optical transition, A_{eff} is the effective beam area, L_{cell} is the vapor cell length, n_i is the number density, and κ_i^2 is a coupling that depends on light detuning and the angular-momentum quantum number. $\Gamma = 1/T_2$ is the spin relaxation rate, related to the FWHM of the noise spectrum by $\Delta\nu = 1/(\pi T_2)$, and given by [35]

$$\frac{1}{T_2} = \Gamma_0 + \alpha n + \beta P, \quad (3)$$

where Γ_0 is the unperturbed linewidth, $n = n_{85} + n_{87}$ is the total atomic density, and α and β are collisional-broadening and power-broadening factors, respectively.

From Eq. (2) we see that it is in principle possible to increase η by increasing either the optical probe power or the atomic density. However both of these actions result in additional broadening of the linewidth $\Delta\nu$. Because one main use of SNS is to measure relaxation processes in an unperturbed spin system [5,6], this additional broadening represents a systematic shift of the measured variable (the linewidth) [17]. On the other hand, Eqs. (2) and (3) predict that squeezing boosts η without additional shifts, providing a quantum advantage irrespective of the other experimental parameters.

III. EXPERIMENT

The experimental setup is shown schematically in Fig. 1(a). A polarization-squeezed probe beam is generated as in [36] by combining local oscillator (LO) laser light with orthogonally polarized squeezed vacuum using a parametric oscillator described in [37], cavity locking system as in [38], and a quantum noise lock (to ensure the measured Stokes component is the squeezed component) described in [33,39]. The probe frequency is stabilized to 20 GHz to the blue of the ^{85}Rb D_1 unshifted line using the system of [40]. Adjusting the LO power changes the probe power P without changing the degree of squeezing. To perform conventional FR-SNS with the coherent LO [3] we simply turn off the squeezer. The effective size of the probe beam, as defined in the Appendix, is 0.054cm^2 .

The atomic system consists of an ovenized cylindrical vapor cell of length $L_{\text{cell}} = 3$ cm and diameter $d = 1$ cm, with natural isotopic abundance Rb and 100 Torr of N_2 buffer gas. Density is controlled by oven temperature and calibrated by absorption at 20 GHz detuning. We alternate 5-s acquisition periods with electrical heating of the oven. Before the cell, measured squeezing at a sideband frequency of 40 kHz is 3.0 dB, while squeezing after the cell ranges from 2.6 to 1.5 dB at the highest density. These numbers are consistent with the expected loss of squeezing due to absorption of the off-resonance probe (see Appendix).

We apply a transverse dc field $B_x = 5.6\ \mu$T and minimize the gradient $\partial B_x/\partial z$ by minimizing the width of the SNS resonances. The oven and coils are inside four layers of high-
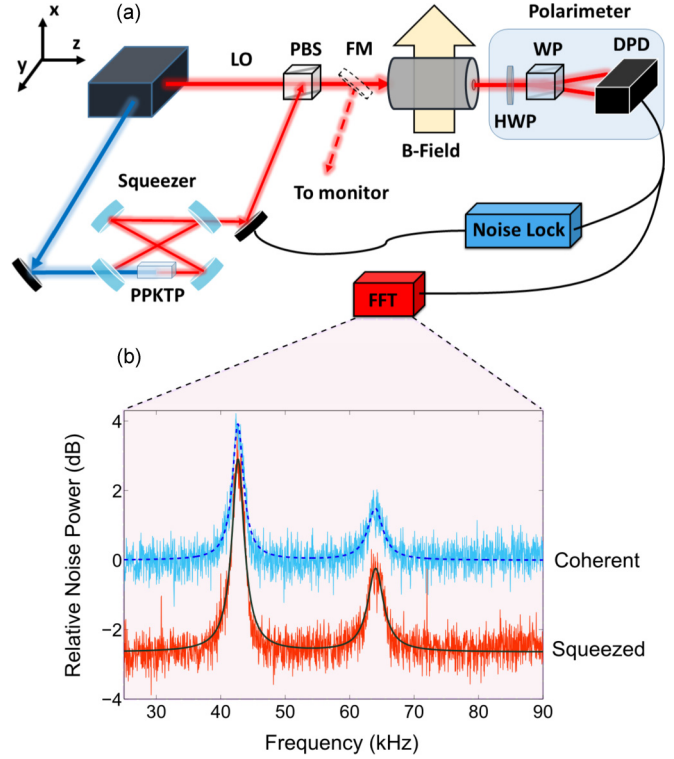

FIG. 1. Squeezed-light spin noise spectroscopy. (a) Experimental schematic. LO - local oscillator, PBS - polarizing beam splitter, DPD - differential photodetector, FM - flip mirror, HWP - half-wave plate, WP - Wollaston prism, FFT - fast Fourier transform analyzer. (b) SNS spectra. Averaged spin noise spectra at $T = 90°$ ($n = 2.4 \times 10^{12}$ cm^{-3}) acquired with coherent probe, cyan (light gray), and polarization squeezed probe, red (dark gray), respectively. The spectra shown are averages of 10 spectra, each representing 0.5 s of acquisition organized into bins of width 10 Hz. 0 dB on the power scale corresponds to -95.57 dBV/Hz at the detector. Dashed and continuous smooth curves show fits by Eq. (1) to the coherent and squeezed spectra, respectively. Optical power $P = 2.5$ mW, magnetic field $B_x = 5.6\ \mu$T.

permeability magnetic shielding. We detect the probe beam with a polarimeter consisting of a half-wave plate, Wollaston prism, and differential photodetector (DPD). The output is recorded by a 24-bit digitizer with 200-kHz sampling rate, and a PC computes the power spectrum.

In Fig. 1(b) we show typical spectra using coherent and polarization squeezed probes. As expected from Eq. (1) we observe the two atomic noise contributions from ^{85}Rb and ^{87}Rb centered at Larmor frequencies ν_L^{85} and ν_L^{87} above a uniform shot noise background. Squeezing reduces the shot noise level without evident change to the spin noise contribution, resulting into a SNR improvement.

IV. DATA ANALYSIS AND RESULTS

At any given optical power and atomic density we acquire 100 individual spin noise spectra as described in Fig. 1(b) and fit them with Eq. (1) to obtain the parameters S_{ph} and $S_{\text{at}}^{(i)}$, $\nu_L^{(i)}$, $\Delta\nu_{(i)}$, and the derived $\eta = S_{\text{at}}^{(i)}/S_{\text{ph}}$, for $i \in \{85,87\}$. Due to imperfect stability of the quantum noise lock, it is necessary to reject about 10% of the traces, identified by the condition

$\chi \equiv \int d\nu \, S(\nu) > 1.03\bar{\chi}$, where the integral is taken over a featureless window between 80 and 90 kHz, not included in the fitting, and $\bar{\chi}$ is the average of χ over the 100 spectra.

In Fig. 2 we show measured ^{85}Rb SNR versus n, the Rb number density, for coherent and squeezed probes at $P = 500\,\mu$W and $P = 4$ mW, which bound our investigated power range, and at the intermediate $P = 1.5$ mW. The temperature range is $T = 85\,^{\circ}$C–120 $^{\circ}$C. As expected from Eq. (2), the SNR increases with both increasing density and increasing power. Squeezing enhances the SNR by a factor ranging from 2.6 dB at $n = 1.5 \times 10^{12}$ cm^{-3} to 1.5 dB at $n = 1.3 \times 10^{13}$ cm^{-3}, with the difference due to greater absorption at higher density. This latter number is higher than the densities used in other alkali SNS works [5,6,18], and at this density we observe collisional broadening $\alpha n/(2\pi) = 760$ Hz, larger than $\Gamma_0/(2\pi) = 501$ Hz. We are thus in a regime where a feature of interest (the linewidth) is already strongly disturbed. Analogous observations apply to the investigated probe power range. In this sense the regime we investigate is fully practical for SNS applications [3,4]. Moreover, the model described in the Appendix shows that the benefit of squeezing extends until the optical absorption becomes strong and the squeezing is lost. The theoretical SNR for squeezed and coherent probes (curves of Fig. 2) converge at a density of $n \approx 1.3 \times 10^{14}$ cm^{-3} (temperature larger than $T = 160^{\circ}$), much above the investigated and practical range of interest. This is our first main result: polarization squeezing significantly improves the SNR of SNS over the full practical range of power and density without any detrimental effect.

Furthermore, in Fig. 3 we show ^{85}Rb SNR η_{85} and FWHM linewidth $\Delta\nu_{85}$ versus optical power for three different experimental situations: $n = 0.5 \times 10^{13}$ cm^{-3} (squeezed only)

FIG. 3. Collisional-broadening reduction. (a) SNR η versus optical power for coherent (empty black squares) and polarization squeezed (filled red circles) probing at $n = 0.9 \times 10^{13}$ cm^{-3} and just for squeezed probe (filled blue circles) at lower density $n = 0.5 \times 10^{13}$ cm^{-3}. Theoretical SNR from Eq. (2) is shown for coherent (dashed lines) and squeezed (continuous lines) probing. (b) FWHM linewidth $\Delta\nu_{85}$ vs probe power for the same conditions of (a). Theoretical FHWM widths from Eq. (3) are plotted for coherent (dashed line) and squeezed (continuous line) probing, respectively.

and, with roughly twice the density, at $n = 0.9 \times 10^{13}$ cm^{-3} (coherent and squeezed). At the higher density, squeezing improves the SNR with respect to the coherent probe without significantly changing the linewidth. At the lower density, squeezing gives the same SNR as the coherent probe gives with the higher density, but with significantly less perturbation of the linewidth. These behaviors are observed over the full investigated power range.

A similar behavior occurs if we compare SNR and linewidth versus atomic density at different probe power levels. Fig. 3(a) already shows that squeezing allows us to get the same classical SNR by using about half of the power, resulting in a reduced power broadening. For completeness, in Fig. 4 we show the FWHM linewidth versus Rb density for $P = 2$ mW and $P = 4$ mW where the SNR with squeezing at $P = 2$ mW is equal to the SNR with coherent probing at $P = 4$ mW. The linewidth reduction with power is smaller than that seen in Fig. 3(b), because the collisional broadening is greater than the broadening due to probe scattering and, in these experimental conditions, dominates the broadening.
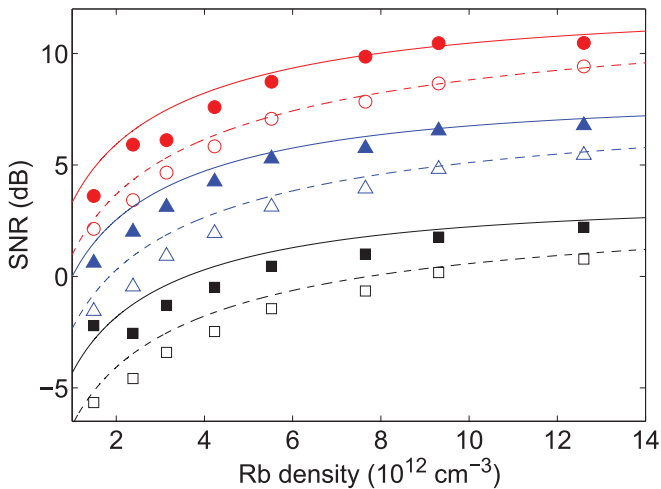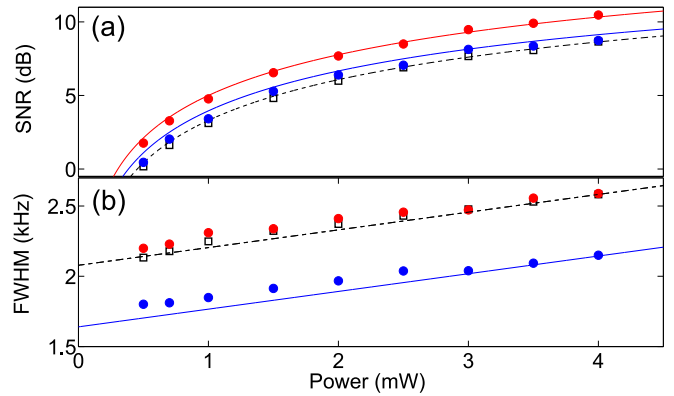

FIG. 2. SNR Enhancement. SNR η versus atomic density for coherent probes (empty markers) and polarization squeezed probes (filled markers). We show three optical powers of $P = 0.5$ mW (squares), $P = 1.5$ mW (triangles), and $P = 4$ mW (circles). Predicted η from Eq. (2) is plotted for coherent (dashed lines) and squeezed (continuous lines) probing, taking into account the reduction of squeezing versus density due to absorption at the probe frequency. The discrepancy between theoretical curves and experimental data is due to uncertainty on density estimation (see Appendix).
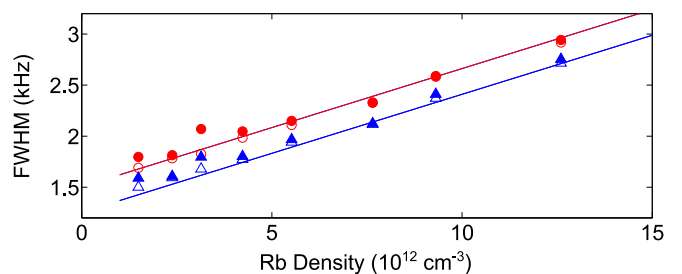

FIG. 4. Power-broadening reduction. FWHM linewidth $\Delta\nu_{85}$ vs Rb density for coherent (empty markers) and polarization squeezed (filled markers) probing at optical powers of $P = 4$ mW (red circles) and $P = 2$ mW (blue triangles). Theoretical FHWM widths from Eq. (3) are plotted.

In Figs. 3 and 4 we show our second main result: squeezing can reduce broadening effects at no cost to figures of merit such as statistical sensitivity.

V. CONCLUSIONS AND OUTLOOK

We have studied the application of polarization-squeezed light to spin noise spectroscopy of atomic ensembles over the full practical range of density and probe power. We observe that squeezing improves the signal-to-noise ratio by an amount comparable to the applied squeezing, in contrast to prior experiments [31] that showed the opposite behavior: increased measurement noise due to squeezing above a critical density. We demonstrate that by using a crystal-based squeezer and off-resonant probing of an unpolarized ensemble, differently from [30,31], optical and atomic quantum noise add incoherently without any coupling. Moreover, squeezing improves the tradeoff between statistical noise and line broadening by giving performance not available with classical probes at any power level.

Our results provide clear evidence that squeezing can improve Faraday-rotation-based SNS measurements, with a broad range of applications in atomic and solid-state physics [3,4]. This advantage over the full practical parameter range for SNS is promising for similar advantages in high-performance magnetometers, gravimeters, and clocks.

ACKNOWLEDGMENTS

APPENDIX

In what follows we present expressions for the shot noise background S_{ph} and the height of the Lorentzian spin noise $S_{at}^{(i)}$ appearing in the function used to fit the power spectral density (PSD) of the polarimeter output as described in the main text. Using these expressions we obtain the SNR $\eta_i = S_{at}^{(i)}/S_{ph}$ [i.e., Eq. (2)] which is used to estimate η for ^{85}Rb as a function of probe light power and density (see solid and dashed lined in Figs. 2 and 3). In generating these estimates we have used the parameters quoted in Table I.

1. Detector signal

In our experiments we analyze $S(\nu)$, the power spectral density of V_{DPD}, which is the output voltage of the polarimeter. Because the scalar signal is acquired by combining polarization rotation information over $\mathcal{A}$, the area of the beam, we write the signal as

$$V_{DPD}(t) = 2G \Re[P \Theta_{FR}(t) + P_{SN}(t)], \quad (A1)$$

where $G = 10^6$ V/A is the transimpedance gain, $P = \int_{\mathcal{A}} dx\, dy\, \mathcal{I}(x,y)$ is the total power of the beam reaching the

TABLE I. Parameters used in computing η. See text for details.

Parameter	Value	Unit
Q	0.87	–
$\alpha/(2\pi)$	57.8	Hz/(10^{12}cm^{-3})
$\beta/(2\pi)$	63	Hz/mW
$\Gamma_0/2\pi$	501	Hz
σ_0	2.4×10^{-12}	cm^2
κ^2	5.0×10^{-4}	–
A_{eff}	0.0544	cm^2
$\Delta\nu_{light}$	2.4	GHz

detector with intensity $\mathcal{I}(x,y)$, and $\Theta_{FR} \ll 1$ is the Faraday rotation (FR) angle as defined in Eq. (A4) below. $\Re = Qq/E_{ph}$ is the detector responsivity, where Q denotes the quantum efficiency of the detector, $E_{ph} = \hbar\omega = 2.4910^{-19}$J is the photon energy at 795 nm, and $q = 1.6 \times 10^{-19}$ C. P_{SN} is a white-noise component due to shot noise, which we now compute.

2. Photon shot noise

The contribution from photon shot noise to $S(\nu)$ is given by

$$S_{ph} = 2G^2 q(\Re P)\xi^2, \quad (A2)$$

where ξ^2 represents the light-squeezing parameter. Figure 5 shows S_{ph}, as estimated by fitting the measured PSD to Eq. (1), at different atomic densities for a coherent probe (hollow symbols) and squeezed probe (filled symbols). The dashed lines and solid lines in Fig. 5 correspond to a fit of the data using Eq. (A2), with Q and ξ^2 as the free parameter in the fit for coherent-probe and squeezed-probe data, respectively. From the coherent-probe data, for which $\xi^2 = 1$, we obtain $Q = 0.87$. The different slopes observed for the squeezing-probe data can be explained by the degradation
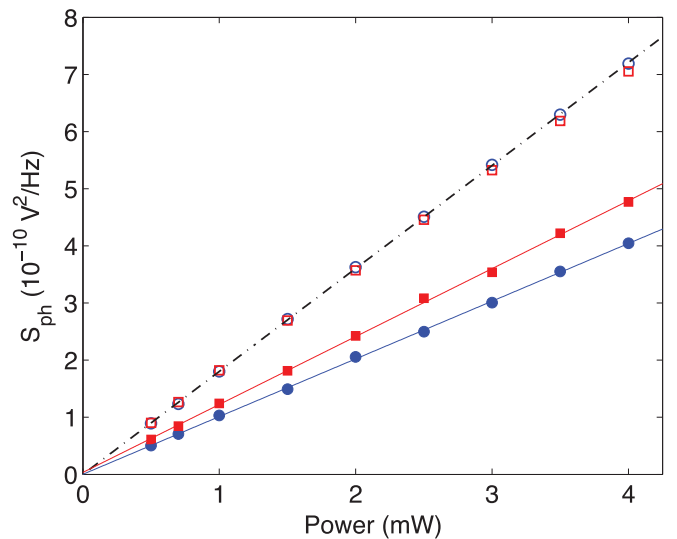

FIG. 5. Shot-noise background, S_{ph}, as a function of probe power reaching the detector for coherent probe (hollow symbols) and squeezed probe (filled symbols) at densities of 2.4×10^{12} cm^{-3} (blue) and 9.3×10^{12} cm^{-3} (red).

of squeezing due to light absorption, given by [25]

$$\xi^2 = 1 - \left(1 - \xi_0^2\right)\exp[-\tau], \quad (A3)$$

where τ is the optical depth experienced by the light beam. For our experimental conditions $\xi_0^2 = 0.55$, obtained by fitting the measured ξ^2 to Eq. (A3) and can be considered as the squeezing parameter of the transmitted light when the cell is at room temperature.

3. Atomic noise

We can compute Θ_{FR} by a coarse-grained approach. Dropping the t for simplicity, and labeling by i the isotope mass number and by j the hyperfine state, so that $f^{(i,j)}$ is the single-atom total spin quantum number, the contribution to Θ_{FR} from atoms in a small region of dimensions $\Delta x \times \Delta y \times L_{cell}$, centered on (x_m, y_m), becomes

$$\Theta_{FR}^{(i,j)} = \frac{1}{P}\frac{D_i(\nu')}{(2I_i+1)}\sum_m P(x_m,y_m)\frac{\sigma_0}{\Delta x \Delta y}F_z^{(i,j,m)}, \quad (A4)$$

where $P(x_m,y_m) \approx \Delta x \Delta y \mathcal{I}(x_m,y_m)$ is the power of the beam in the given region, $2I_i + 1$ is a geometrical factor accounting for the hyperfine coupling between electronic spin ($S = 1/2$) and nuclear spin (I_i) of the atom, so that $f^{(i,j)} = I_i + j$, $j \in \{-\frac{1}{2},+\frac{1}{2}\}$, and $F_z^{(i,j,m)}$ is the z component of the collective angular momentum operator, i.e., the sum of the individual angular momenta $\mathbf{f}^{(i,j)}$ for atoms in the given region.

The on-resonance cross section for the collision-broadened optical line is [41]

$$\sigma_0 = \frac{c r_e f_{osc}}{\Delta\nu_{light}/2} = 2.4 \times 10^{-12} \text{ cm}^2, \quad (A5)$$

where $r_e = 2.82 \times 10^{-13}$ cm is the classical electron radius, $f_{osc} = 0.34$ is the oscillator strength of the D_1 transition in Rb, and c is the speed of light. The spectral factor is

$$D_i(\nu') = \frac{(\nu'-\nu_j')\Delta\nu_{light}/2}{(\nu'-\nu_j')^2+(\Delta\nu_{light}/2)^2}, \quad (A6)$$

where ν' and ν_j', denote the probe optical frequency and optical resonance frequency, respectively, and $\Delta\nu_{light}$ represents the pressure-broadened FWHM of the optical transition. For the vapor cell used in our experiments $\Delta\nu_{light} \approx 2.4$ GHz due to 100 Torr of N_2 buffer gas.

For a given region, the mean of the collective spin projection is $\langle F_z^{(i,j,m)}\rangle = n_i \Delta x \Delta y L_{cell} \text{Tr}[\rho f_z^{i,j}] = 0$ where n_i is the atomic density of the ith species, and ρ is the thermal state, which to a very good approximation is a uniform mixture of the ground states. As a result $\langle\Theta_{FR}^{(i,j)}\rangle = 0$.

In a similar way, and assuming that different atoms are independent, so that their variances sum, we find

$$\text{var}\Theta_{FR}^{(i,j)} = \left(\frac{\sigma_0}{P}\frac{D_i(\nu')}{(2I_i+1)}\right)^2 \text{var}\sum_m \mathcal{I}(x_m,y_m)F_z^{(i,j,m)}$$

$$\propto \sum_m \text{var}\mathcal{I}(x_m,y_m)F_z^{(i,j,m)}$$

$$\propto \sum_m \mathcal{I}^2(x_m,y_m)\text{var}F_z^{(i,j,m)}, \quad (A7)$$

where $\text{var}F_z^{(i,j,m)} = n_i\,\Delta x\,\Delta y\,L_{cell}\text{Tr}[\rho(f_z^{(i,j)})^2]$, with

$$\text{Tr}\left[\rho\left(f_z^{(i,j)}\right)^2\right] = \frac{f^{(i,j)}(f^{(i,j)}+1)(2f^{(i,j)}+1)}{6(2I_i+1)}. \quad (A8)$$

Taking the limit $\Delta x \Delta y \to dx\,dy$, and assuming the contributions of different isotopes and different hyperfine levels contribute independently, the spin noise due to isotope i is

$$\text{var}\Theta_{FR}^{(i)} = \kappa_i^2\sigma_0^2 n L_{cell}\frac{\int dx\,dy\mathcal{I}^2(x,y)}{P^2}, \quad (A9)$$

where the parameter κ_i^2 is given by

$$\kappa_i^2 = \sum_j \frac{D_i^2(\nu')}{(2I_i+1)^3}\frac{f^{(i,j)}(f^{(i,j)}+1)(2f^{(i,j)}+1)}{6}. \quad (A10)$$

Equation (A9) is conveniently expressed as

$$\text{var}\Theta_{FR}^{(i)} = N_i\frac{\sigma_0^2}{A_{eff}^2}\kappa_i^2, \quad (A11)$$

where $N_i \equiv n_i A_{eff} L_{cell}$ is the effective number of isotope-i atoms in the beam, and A_{eff} is the effective area [27]:

$$A_{eff} \equiv \frac{[\int dx\,dy\,\mathcal{I}(x,y)]^2}{\int dx\,dy\,\mathcal{I}^2(x,y)}. \quad (A12)$$

The spin noise oscillates at the Larmor frequency ν_i and with FWHM linewidth $\Delta\nu_i$, so that

$$S(\nu) = S_{ph} + \sum_{i\in\{85,87\}} S_{at}^{(i)}\frac{(\Delta\nu/2)^2}{(\nu-\nu_i)^2+(\Delta\nu/2)^2}, \quad (A13)$$

where

$$S_{at}^{(i)}(\nu) = \frac{4G^2\mathfrak{R}^2P^2}{\pi\Delta\nu/2}\text{var}\Theta_{FR}^{(i)}. \quad (A14)$$

From the fitted amplitude $S_{at}^{(85)}$ and FWHM $\Delta\nu_{85}$ of the Rb^{85} spin noise spectrum, we compute $\text{var}\Theta_{FR}^{(85)}$ using Eq. (A14). These data are shown in Fig. 6 as a function of the Rb-vapor

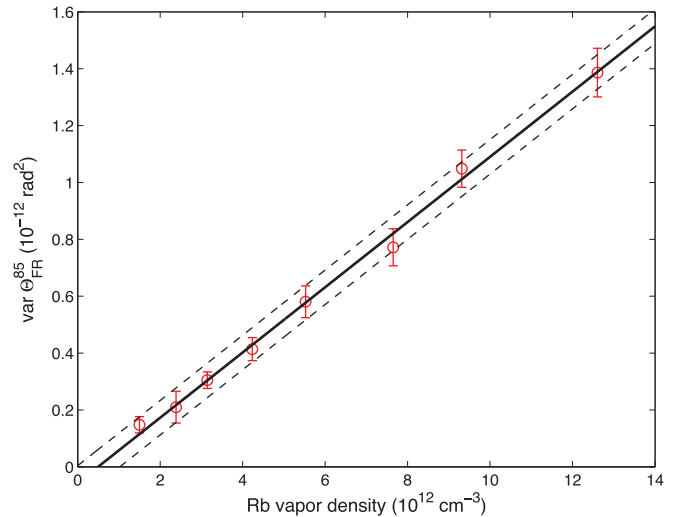FIG. 6. Var $\Theta_{FR}^{(85)}$ as a function of atomic density for coherent probe. The solid line shows a linear fit to the data. Dashed lines show the best fit $\pm 3\sigma$ statistical uncertainty in the fit offset.

density n. The solid line in Fig. 6 corresponds to a fit of the data using Eq. (A11) with κ_{85}^2 as the free parameter and with $N_{85} = 0.72 n A_{\rm eff} L_{\rm cell}$, here $A_{\rm eff} = 0.054 \, {\rm cm}^2$ and $L_{\rm cell} = 3 \, {\rm cm}$. From the fit we obtain $\kappa_{85}^2 = 5 \times 10^{-4}$, to be compared with the value of 3.7×10^{-4} obtained by evaluating Eq. (A10) with a detuning of $\nu' - \nu'_{85} = 20 \, {\rm GHz}$ and optical linewidth $\Delta \nu_{\rm light} = 2.4 \, {\rm GHz}$, and using $\sigma_0 = 2.4 \times 10^{-12} \, {\rm cm}^2$.

4. Width of the magnetic line

For ^{85}Rb the FWHM width of the magnetic line is $\Delta \nu = 1/(\pi T_2)$, and can be approximated by [35]

$$\frac{1}{T_2} = \Gamma_0 + \alpha n + \beta P, \tag{A15}$$

where αn and βP are the contributions from atomic collisions and power broadening, respectively, with n being the Rb-vapor density, P the optical power of the probe beam, and Γ_0 the spin relaxation due to other mechanisms, including buffer-gas collisions and the finite residence time of the atoms in the light beam.

To estimate the power-broadening and collisional-broadening parameters we fit the measured $\Delta \nu_{85}$ using Eq. (A15). From the fit we obtain a collisional-broadening parameter $\alpha/(2\pi) = 57.8 \, {\rm Hz}/(10^{12} \, {\rm cm}^{-3})$, a power-broadening parameter $\beta/(2\pi) = 63 \, {\rm Hz/mW}$, and $\Gamma_0/(2\pi) = 501 \, {\rm Hz}$.

5. SNR

Using Eqs. (A2), (A11), (A14), and (A15) we obtain the following expression for the SNR $\eta_i \equiv S_{\rm at}^{(i)}/S_{\rm ph}$

$$\eta_i = \frac{P}{\hbar\omega} \frac{4Q}{\xi^2} \frac{\sigma_0^2}{A_{\rm eff}^2} \frac{\kappa_i^2 N_i}{\Gamma}, \tag{A16}$$

where $N_i = n_i A_{\rm eff} L_{\rm cell}$, thus arriving at Eq. (2).

[1] F. Bloch, Phys. Rev. **70**, 460 (1946).

[2] B. Aleksandrov and V. S. Zapasskii, Sov. Phys. JETP **54**, 64 (1981).

[3] V. S. Zapasskii, Adv. Opt. Photon. **5**, 131 (2013).

[4] J. Hübner, F. Berski, R. Dahbashi, and M. Oestreich, Phys. Status Solidi B **251**, 1824 (2014).

[5] S. A. Crooker, D. G. Rickel, A. V. Balatsky, and D. L. Smith, Nature **431**, 49 (2004).

[6] G. E. Katsoprinakis, A. T. Dellis, and I. K. Kominis, Phys. Rev. A **75**, 042502 (2007).

[7] M. Oestreich, M. Römer, R. J. Haug, and D. Hägele, Phys. Rev. Lett. **95**, 216603 (2005).

[8] M. Römer, J. Hübner, and M. Oestreich, Appl. Phys. Lett. **94**, 112105 (2009).

[9] Q. Huang and D. S. Steel, Phys. Rev. B **83**, 155204 (2011).

[10] F. Berski, H. Kuhn, J. G. Lonnemann, J. Hübner, and M. Oestreich, Phys. Rev. Lett. **111**, 186602 (2013).

[11] S. V. Poltavtsev, I. I. Ryzhov, M. M. Glazov, G. G. Kozlov, V. S. Zapasskii, A. V. Kavokin, P. G. Lagoudakis, D. S. Smirnov, and E. L. Ivchenko, Phys. Rev. B **89**, 081304 (2014).

[12] S. A. Crooker, J. Brandt, C. Sandfort, A. Greilich, D. R. Yakovlev, D. Reuter, A. D. Wieck, and M. Bayer, Phys. Rev. Lett. **104**, 036601 (2010).

[13] Y. Li, N. Sinitsyn, D. L. Smith, D. Reuter, A. D. Wieck, D. R. Yakovlev, M. Bayer, and S. A. Crooker, Phys. Rev. Lett. **108**, 186603 (2012).

[14] R. Dahbashi, J. Hübner, F. Berski, K. Pierz, and M. Oestreich, Phys. Rev. Lett. **112**, 156601 (2014).

[15] V. S. Zapasskii, A. Greilich, S. A. Crooker, Y. Li, G. G. Kozlov, D. R. Yakovlev, D. Reuter, A. D. Wieck, and M. Bayer, Phys. Rev. Lett. **110**, 176601 (2013).

[16] L. Yang, P. Glasenapp, A. Greilich, D. Reuter, A. D. Wieck, D. R. Yakovlev, M. Bayer, and S. A. Crooker, Nat. Commun. **5**, 4949 (2014).

[17] P. Glasenapp, N. A. Sinitsyn, L. Yang, D. G. Rickel, D. Roy, A. Greilich, M. Bayer, and S. A. Crooker, Phys. Rev. Lett. **113**, 156601 (2014).

[18] A. T. Dellis, M. Loulakis, and I. K. Kominis, Phys. Rev. A **90**, 032705 (2014).

[19] D. Roy, L. Yang, S. A. Crooker, and N. A. Sinitsyn, Sci. Rep. **5**, 9573 (2015).

[20] T. Sleator, E. L. Hahn, C. Hilbert, and J. Clarke, Phys. Rev. Lett. **55**, 1742 (1985).

[21] W. Reim, R. H. Koch, A. P. Malozemoff, M. B. Ketchen, and H. Maletta, Phys. Rev. Lett. **57**, 905 (1986).

[22] D. Rugar, R. Budakian, H. J. Mamin, and B. W. Chui, Nature **430**, 329 (2004).

[23] R. Budakian, H. J. Mamin, B. W. Chui, and D. Rugar, Science **307**, 408 (2005).

[24] C. L. Degen, M. Poggio, H. J. Mamin, and D. Rugar, Phys. Rev. Lett. **99**, 250601 (2007).

[25] J. L. Sørensen, J. Hald, and E. S. Polzik, Phys. Rev. Lett. **80**, 3487 (1998).

[26] G. M. Müller, M. Oestreich, M. Römer, and J. Hübner, Phys. E (Amsterdam, Neth.) **43**, 569 (2010).

[27] V. Shah, G. Vasilakis, and M. V. Romalis, Phys. Rev. Lett. **104**, 013601 (2010).

[28] S. Li, P. Vachaspati, D. Sheng, N. Dural, and M. V. Romalis, Phys. Rev. A **84**, 061403 (2011).

[29] P. Glasenapp, A. Greilich, I. I. Ryzhov, V. S. Zapasskii, D. R. Yakovlev, G. G. Kozlov, and M. Bayer, Phys. Rev. B **88**, 165314 (2013).

[30] I. Novikova, E. E. Mikhailov, and Y. Xiao, Phys. Rev. A **91**, 051804 (2015).

[31] T. Horrom, R. Singh, J. P. Dowling, and E. E. Mikhailov, Phys. Rev. A **86**, 023803 (2012).

[32] D. Budker and M. Romalis, Nat. Phys. **3**, 227 (2007).

[33] F. Wolfgramm, A. Cerè, F. A. Beduini, A. Predojević, M. Koschorreck, and M. W. Mitchell, Phys. Rev. Lett. **105**, 053601 (2010).

[34] V. G. Lucivero, P. Anielski, W. Gawlik, and M. W. Mitchell, Rev. Sci. Instrum. **85**, 113108 (2014).

[35] R. Jiménez-Martínez, W. C. Griffith, S. Knappe, J. Kitching, and M. Prouty, J. Opt. Soc. Am. B **29**, 3398 (2012).

[36] P. Grangier, R. E. Slusher, B. Yurke, and A. LaPorta, Phys. Rev. Lett. **59**, 2153 (1987).

[37] A. Predojevic, Z. Zhai, J. M. Caballero, and M. W. Mitchell, Phys. Rev. A **78**, 063820 (2008).

[38] F. A. Beduini, J. A. Zielińska, V. G. Lucivero, Y. A. de Icaza Astiz, and M. W. Mitchell, Phys. Rev. Lett. **113**, 183602 (2014).

[39] K. McKenzie, E. E. Mikhailov, K. Goda, P. K. Lam, N. Grosse, M. B. Gray, N. Mavalvala, and D. E. McClelland, J. Opt. B **7**, S421 (2005).

[40] J. Kong, V. G. Lucivero, R. Jiménez-Martínez, and M. W. Mitchell, Rev. Sci. Instrum. **86**, 073104 (2015).

[41] W. Happer, Y.-Y. Jau, and T. Walker, *Optically Pumped Atoms* (Wiley, New York, 2010).